

**Zeitschrift:** IABSE publications = Mémoires AIPC = IVBH Abhandlungen  
**Band:** 30 (1970)  
  
**Artikel:** Mild steel beams under cyclic alternating deflections  
**Autor:** Sherbourne, A.N. / Krishnasamy, S.  
**DOI:** <https://doi.org/10.5169/seals-23584>

### **Nutzungsbedingungen**

Die ETH-Bibliothek ist die Anbieterin der digitalisierten Zeitschriften auf E-Periodica. Sie besitzt keine Urheberrechte an den Zeitschriften und ist nicht verantwortlich für deren Inhalte. Die Rechte liegen in der Regel bei den Herausgebern beziehungsweise den externen Rechteinhabern. Das Veröffentlichen von Bildern in Print- und Online-Publikationen sowie auf Social Media-Kanälen oder Webseiten ist nur mit vorheriger Genehmigung der Rechteinhaber erlaubt. [Mehr erfahren](#)

### **Conditions d'utilisation**

L'ETH Library est le fournisseur des revues numérisées. Elle ne détient aucun droit d'auteur sur les revues et n'est pas responsable de leur contenu. En règle générale, les droits sont détenus par les éditeurs ou les détenteurs de droits externes. La reproduction d'images dans des publications imprimées ou en ligne ainsi que sur des canaux de médias sociaux ou des sites web n'est autorisée qu'avec l'accord préalable des détenteurs des droits. [En savoir plus](#)

### **Terms of use**

The ETH Library is the provider of the digitised journals. It does not own any copyrights to the journals and is not responsible for their content. The rights usually lie with the publishers or the external rights holders. Publishing images in print and online publications, as well as on social media channels or websites, is only permitted with the prior consent of the rights holders. [Find out more](#)

**Download PDF:** 09.12.2025

**ETH-Bibliothek Zürich, E-Periodica, <https://www.e-periodica.ch>**

## Mild Steel Beams Under Cyclic Alternating Deflections

*Poutres en acier doux soumises à des flexions cycliques alternées*

*Träger aus normalem Baustahl unter zyklischer Verformung*

A. N. SHERBOURNE

Professor of Civil Engineering and Dean  
of the Faculty of Engineering, University  
of Waterloo, Waterloo, Ontario, Canada

S. KRISHNASAMY

Research Assistant Professor, Department  
of Civil Engineering, University of Water-  
loo, Waterloo, Ontario, Canada

### Introduction

Simple plastic theory is based upon the concept of a set of proportional loads which affect the collapse of a structure. In determining the load, ductility of the material is considered rather than fracture. The theory is, in reality, a limiting strength theory based upon the probability of failure of a structure under a single application of a peak load rather than gradual collapse under repeated application of loads below the static collapse value.

It is seldom, however, that a structure will be subjected to static load only. In its lifetime, it may well suffer variable repeated loading such as wind, snow, etc., even though the periodicity may vary within wide limits. The repeated application of the load may cause the structure to fail either by "incremental collapse" or "alternating plasticity".

The second type of failure is somewhat similar to a fatigue failure but requires a much smaller number of cycles, a higher intensity of alternating loads leading to a greater range of stress and a low frequency of application leading to a longer time at peak values.

Considerable work has been done on the elastic-plastic response of structures and several analytical solutions have been proposed for determining the "shakedown" load. These theoretical studies have often been verified by tests on model and full-scale structures [1-6]. It is important to point out that changes in material properties during cyclic loading are not taken into account in the theoretical analysis of "shakedown" and "incremental collapse load" problems where it is assumed that each application of peak load is sustained



for a sufficiently long period as to allow the deformations of the structure to stabilize; in this sense the loading is presumed to be "quasi-static". It is clear from the published work on the material properties under cyclic loading conditions that there is a significant change in the stress-strain characteristics of the steel from one cycle to the other over a wide range of loading frequencies from very high to quite low. It is necessary, therefore, to account for these changes in material properties in analysing structures under cyclic loading conditions; this is attempted here for low frequencies.

When a structure, loaded beyond the elastic limit, is subjected to cyclic loading at or near the collapse value, the nature of the problem is completely changed. The difference between conventional fatigue and this particular type of problem is that the former is associated with high intensities of loading producing failure after relatively few cycles. It is customary to refer to this second problem as "low endurance" fatigue.

The materials aspect of the "low endurance" problem has been the subject of investigation by many research workers [7-11]. The structural aspect of the problem of "alternating plasticity" has received very little attention [12, 13].

The little work done in this area is inconclusive in helping to predict structural behaviour analytically since no attempt is made to relate dynamic material properties to the study of structural response. The work after ROYLES [14] throws some light on simple and continuous beams under a constant deflection range in formulating empirical moment-curvature relationship for mild steel beams subjected to alternate bending.

The procedure of ROYLES [14] ignores partially the effect of elasticity in constructing the moment-curvature relation or otherwise assumes a fully non-linear material. The application of this type of moment-curvature relation to simple structures, where the major part of the structure is well in the plastic range, will not produce much error. In the case of statically indeterminate structures, however, where the major portion of the structure may remain elastic, the error may be considerable.

The nature of the loading on structures is random, and consequently, it is very difficult to study such a complex problem directly. The problem can be classified into two cases involving (I) load control, and (II) deflection control. Once mathematical models have been established for the above two types it might be possible to formulate a solution for the more general random loading case.

The purpose of this investigation is to develop an analytical technique for deriving the cyclic behaviour of simple structures under a constant range of alternating displacements (strains). It should be emphasized that alternating displacements only are considered, of a type in which the maximum amplitudes are identical in hogging and sagging.

The ambient conditions of loading rate are such as to confine the investiga-

tion to low cyclic fatigue behaviour (1–100 cpm). The method depends upon the generation of “pseudo-static” moment-curvature relationships which are discrete functions of the instantaneous cyclic history. These curves are obtained either from cyclic tests on beams under pure bending or from cyclic “push-pull” tests.

The moment-curvature models are derived from cyclic pure bending tests or “push-pull” tests (controlling the strain range) and are then applied to study the behaviour of structural components under controlled deflection amplitudes of equal and opposite sign. The problem where the deflection is being controlled is neither strain controlled nor load controlled. In fact, when the deflection range at one point is controlled, the strain (curvature) range and the moment (or load) at every other point changes from cycle to cycle because of the varying strain hardening rates under different strain ranges. Hence the analytical technique proposed here can predict the experimental values if the deflected shape of the beam is controlled rather than the peak deflection range at one particular point. In a pure bending (or push-pull) problem, where the strain range is controlled, the moment (or stress) amplitude increases from one cycle to the other; but if the moment (or stress) amplitude is controlled the strain range decreases [14–16]. The exception to the above statement occurs if the controlled range of strain or moment (or stress) is in the region of yield, where the reverse is true. In a situation where all these parameters change and a different parameter of deformation is controlled, it is reasonable to assume that the moment (or stress) will be less than the case where the strain range alone is controlled. Based on this conclusion, and on the fact that the moment-curvature models employed in the calculations are derived from strain controlled tests, it can be deduced that the theory proposed in this paper will yield an upper bound envelope behaviour. On the other hand, the load controlled problem (which is not the subject of this paper) will yield a lower bound “solution”.

### Moment-Curvature Characteristics

Two types of steels are used in the experiments reported in this paper and their chemical compositions are reported here. The material used in pure bending, push-pull and cantilever tests is of the following composition:

Si	S	P	Mn	C	Cr	Fe
0.037	0.025	0.004	0.47	0.143	0.01	Remainder %

The chemical properties of the steel used in four point bending, simple and continuous beam tests are as follows:

C	Mn	S	P	Si	Fe
0.12	0.7	0.05			Remainder %

The cyclic moment-curvature relations for the analysis of structural components can be formulated in two ways from (I) axial push-pull tests, and (II) cyclic reversed (pure) bending tests.

In general, four types of moment-curvature models can be employed in the analysis as follows: (I) the model is linear until yield and non-linear beyond, (II) non-linear from the outset, (III) bi-linear with two different slopes, and (IV) a rigid-strain hardening type. The first two models are employed in the analysis of structural components (determinate and indeterminate) reported in this paper; the first of these two accounts for the effect of elasticity while the second ignores it partly. The third model is similar to the first one except for a constant slope in the non-linear range which is represented by a polynomial in the first case. The fourth model completely ignores the effect of elasticity. All four models are employed on a determinate structure (cantilever beam) and the results are represented together with the experiment on the same plot for the purposes of comparison. The first two models lead to complicated numerical calculations because of their non-linearity, while the latter ones are less cumbersome to apply. It follows, in general, that the Model I will yield values closer to experiments than Model II. In the higher range of strain, however, where the effects of plastic strain dominate, the predictions are almost identical implying that the simpler continuous non-linear model (Model II) can often be employed in the analysis of structures where elastic strains are small compared with inelastic strains. Model III will yield an upper bound solution (as in Model I) but the calculations will be simplified to a significant extent. When the elastic and plastic strains are comparable, the error will be appreciable, but this will diminish as the plastic strain increases compared with elastic strain. In the case of Model IV, since the contribution due to the elastic component is neglected, the error in the working range (where the strains are very small) might be serious. The four moment-curvature models can be represented mathematically as follows in non-dimensional form:

$$\begin{array}{llll} k = m & \text{elastic} & \text{Model I,} & (1) \\ k = 1.0 + \alpha_1(m-1)^{\beta_1} & \text{inelastic} & & \end{array}$$

$$k = \alpha_2(m)^{\beta_2} \quad \text{Model II,} \quad (2)$$

$$\begin{array}{llll} k = m & \text{elastic} & \text{Model III,} & (3) \\ k = C + \alpha_3(m-C) & \text{inelastic} & & \end{array}$$

$$k = \alpha_4(m-m_c) \quad \text{Model IV.} \quad (4)$$

The constants  $\alpha_1$ ,  $\alpha_2$ ,  $\alpha_3$ ,  $\alpha_4$ ,  $\beta_1$ ,  $\beta_2$ ,  $C$  and  $m_c$  are functions of the number of cycles for which the particular model is constructed and can be computed by plotting the appropriate data from the experiments on pure bending specimen or push-pull tests.

From reversed bending tests ROYLES [14] has concluded that the influence

of axial extension is predominant when strain range exceeds  $\pm 2.5\%$  and that moment amplitudes have to be adjusted accordingly. The present study was limited to an inelastic strain range varying from yield to  $\pm 2.5\%$ . In the experiments after ROYLES [14] (also reported here), the maximum strain range considered was  $\pm 5.5\%$ , and the results were adjusted accordingly for the effect of axial extension.

### Push-Pull Tests

The results of cyclic axial push-pull tests [17] are plotted on a log-log scale (Fig. 1). By cross plotting from Fig. 1, the stress-strain curves of Fig. 2a, can be derived for various cycles. The stress-strain expression can be represented by a power law

$$\Delta\sigma = a(\Delta\epsilon)^b, \quad (5)$$

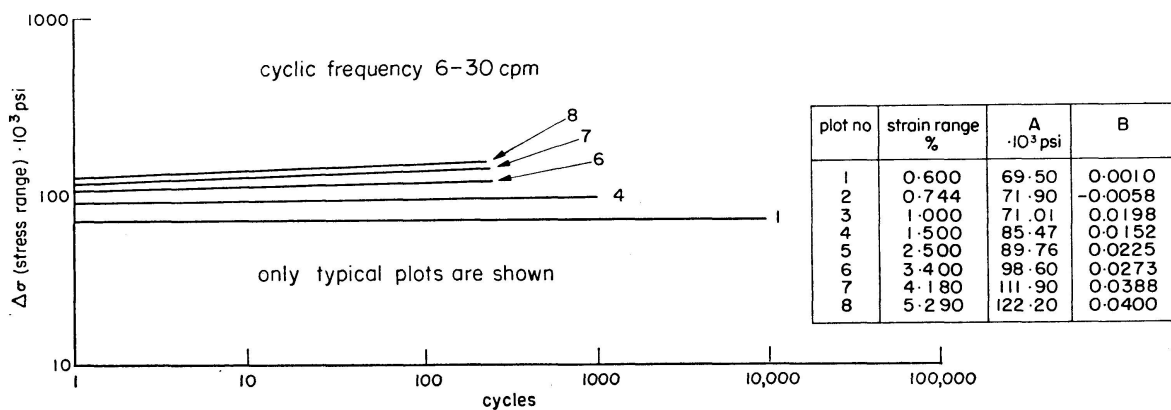


Fig. 1. Cyclic Variation of Stress Range under Constant Strain Cycling.

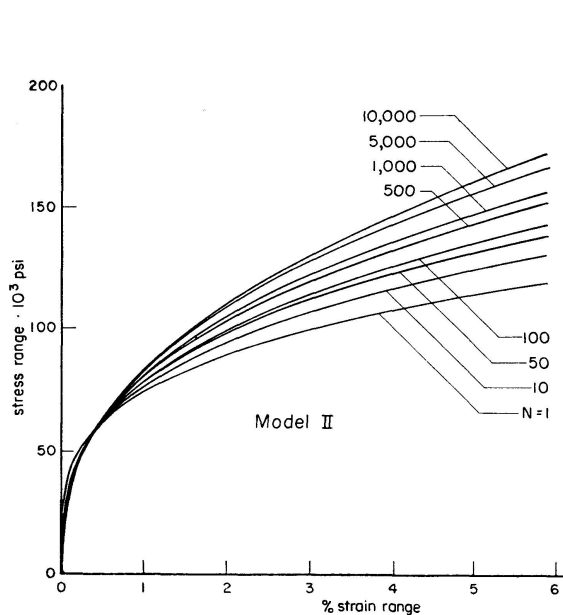


Fig. 2a. Cyclic Stress-Strain Characteristics.

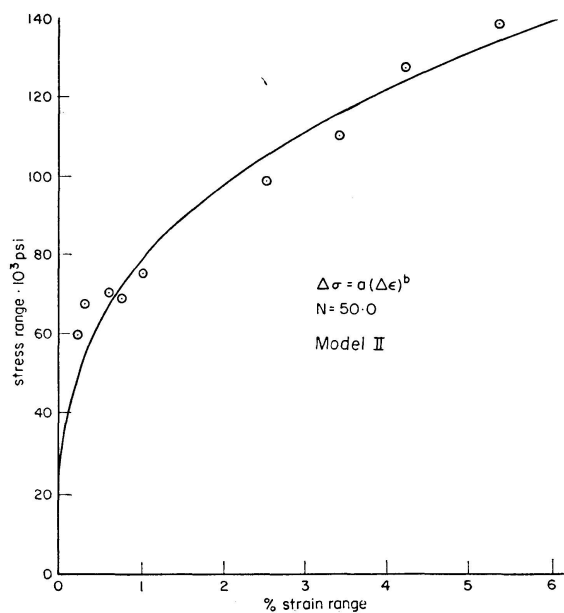


Fig. 2b. Cyclic Stress-Strain Curve: A Typical Value.

Table 1a. (Authors)

Cycles	$\alpha_1$	$\beta_1$	$\alpha_2$	$\beta_2$
1.0	13.0	4.1521	0.22	5.6568
5.0	10.4	3.7020	0.35	4.7976
10.0	9.5	3.145	0.31	4.8692
50.0	8.6	2.604	0.45	4.0885
100.0	8.0	2.550	0.52	3.7934
500.0	7.3	2.26	0.56	3.7399
1000.0	7.0	2.115	0.62	3.5424
5000.0	6.2	1.9678	0.62	3.4306
10000.0	5.8	2.0773	0.64	3.4092

Table 1b. (ROYLES)

Cycles	$\alpha_1$	$\beta_1$	$\alpha_2$	$\beta_2$
1.0	10.980	1.9000	0.9961	3.4622
5.0	9.618	1.9003	0.9548	3.3577
10.0	9.003	1.9087	0.9268	3.3177
50.0	7.852	1.8972	0.8964	3.2041
100.0	7.379	1.8940	0.8833	3.1528
250.0	6.764	1.9002	0.8533	3.1041
500.0	6.348	1.8972	0.8397	3.0542
1000.0	5.964	1.8851	0.8358	2.9903
1600.0	5.720	1.8895	0.8193	2.9723

where  $a$  and  $b$  are material constants for a particular cycle (Table 1a). As seen from Fig. 2b, the power law very closely represents the material behaviour.

The cyclic moment-curvature relations for rectangular sections can be deduced as shown in Appendix I and may be represented in Fig. 3a. In Fig. 3b, the moment-curvature characteristic derived from push-pull tests for a particular cycle is plotted along with the experimental points from pure bending tests. The geometric constants are computed and shown in Table 1b.

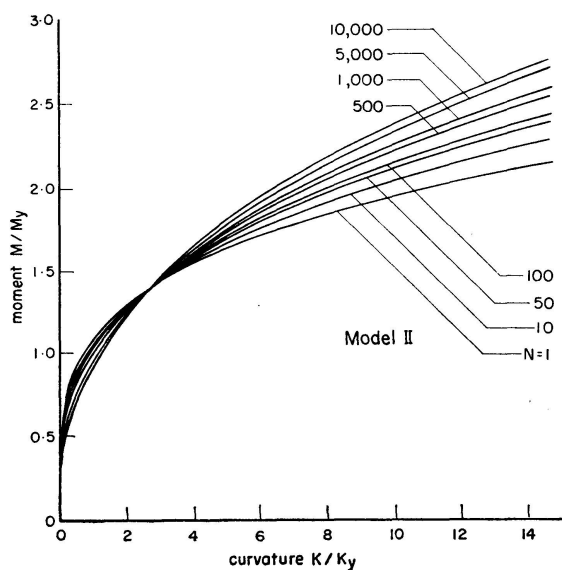


Fig. 3a. Cyclic Moment-Curvature Relationships: From Push-Pull Tests.

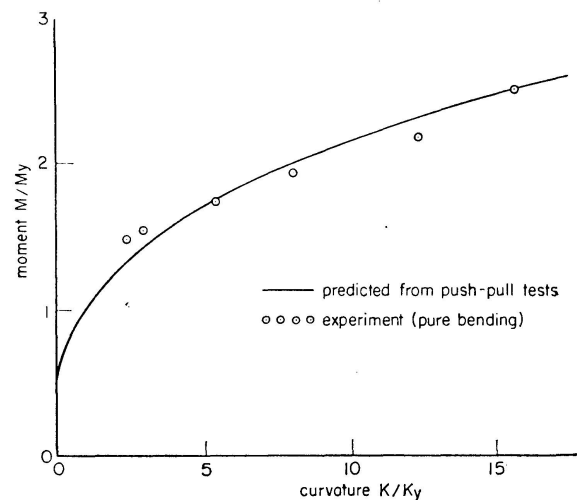


Fig. 3b. Cyclic Moment-Curvature Relationship: A Typical Value ( $N=100.0$ ).

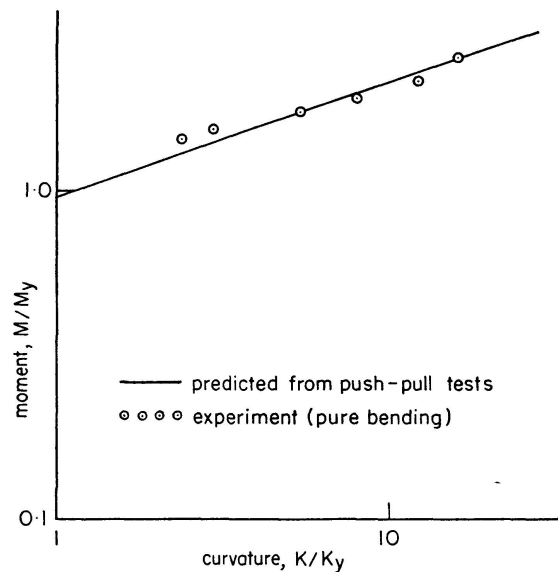


Fig. 3c. Cyclic Moment-Curvature Relationship: Log Scale.

### Pure Bending Tests [19, 20]

The constants  $\alpha_1$ ,  $\alpha_2$ ,  $\alpha_3$ ,  $\alpha_4$ ,  $\beta_1$ ,  $\beta_2$ ,  $C$  and  $m_c$  for various numbers of cycles are computed by plotting the data from Figs. 4 and 5 (see Fig. 6) and listing as indicated in Table 2. The cyclic moment-curvature models generated by employing these constant are shown in Fig. 7 for the first two models used in the analysis. These moment-curvature characteristics are employed to predict analytically the cyclic response of structural components under reversed bending.

Fig. 6a shows the log-log plots of both  $m-k$  models (I and II) for a parti-

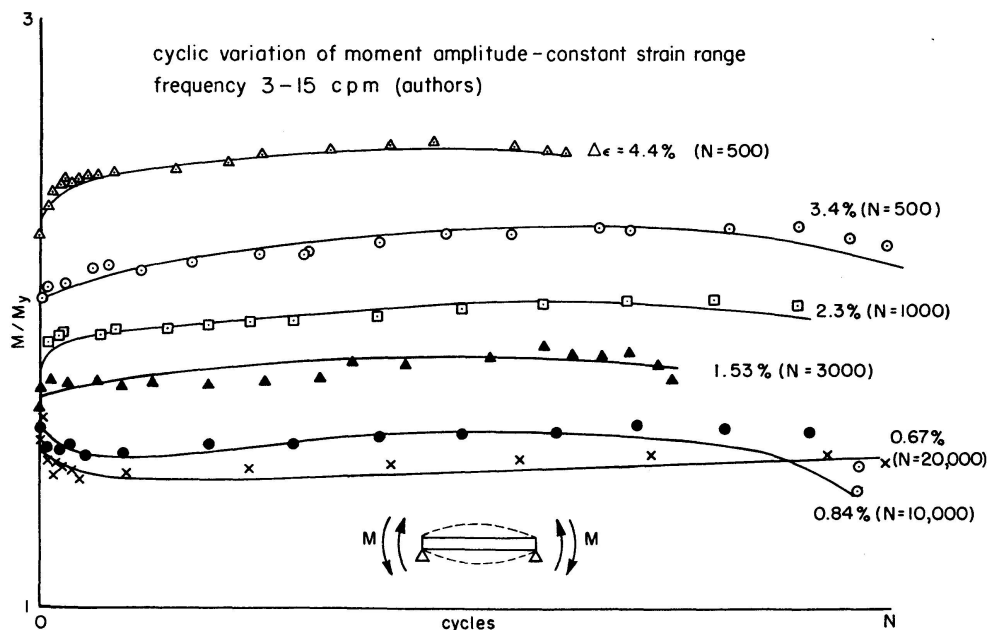


Fig. 4a. Cyclic Variation of Moment Amplitude: Constant Strain Range (Authors).

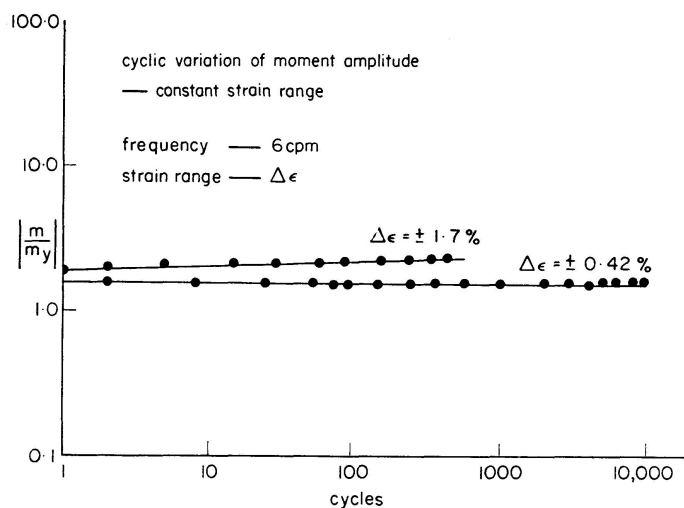


Fig. 4b. Cyclic Variation of Moment Amplitude under Constant Strain Range: Log Scale.

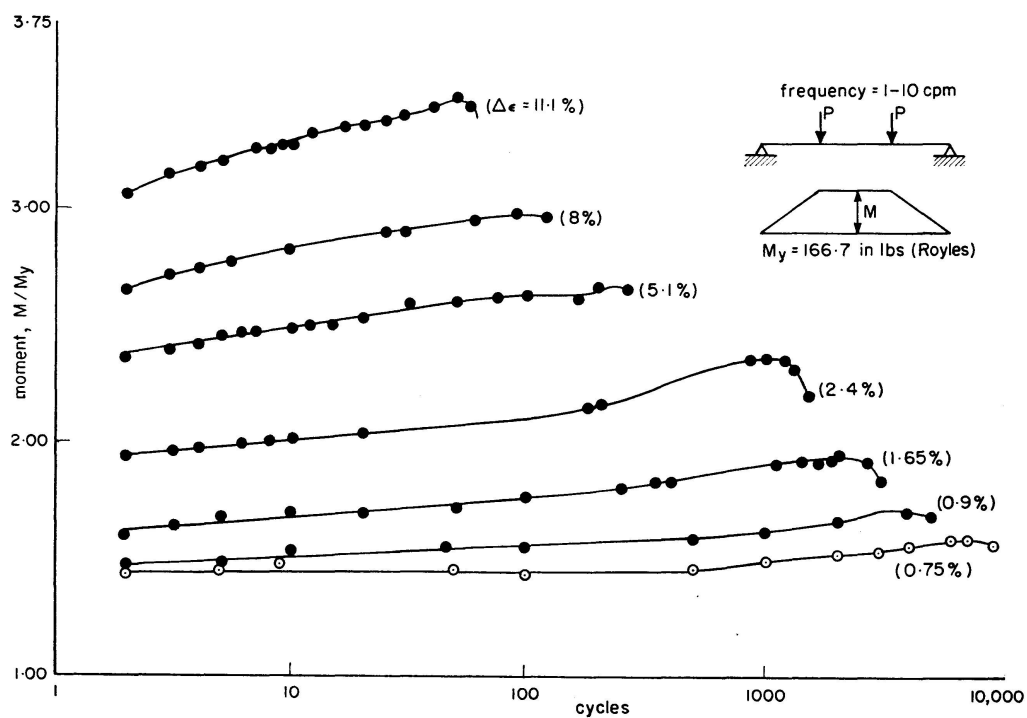


Fig. 5. Cyclic Variation of Moment Amplitude: Constant Strain Range (Royles).

Table 2a

Cycle	$a \times 10^3$ psi.	$b$
1.0	248.6	0.2599
10.0	302.7	0.2968
50.0	347.3	0.3225
100.0	368.4	0.3336
500.0	422.9	0.3594
1000.0	448.6	0.3705
5000.0	514.8	0.3963
10000.0	546.3	0.4073

Table 2b

Cycle	$\alpha_2$	$\beta_2$
1.0	0.7736	3.8476
10.0	0.9022	3.3693
50.0	0.9822	3.1008
100.0	1.0160	2.9976
500.0	1.0870	2.7824
1000.0	1.1160	2.6991
5000.0	1.1800	2.5233
10000.0	1.2040	2.4552

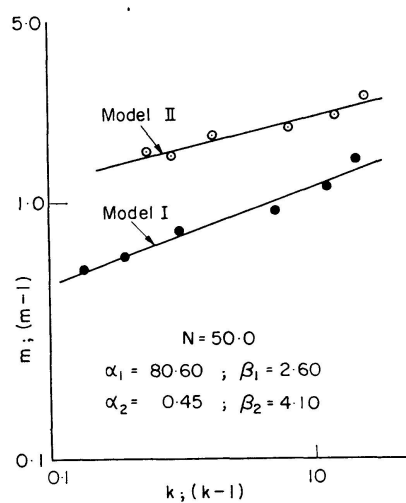


Fig. 6a. Cyclic Moment-Curvature Characteristics (Models I and II): Log Scale.

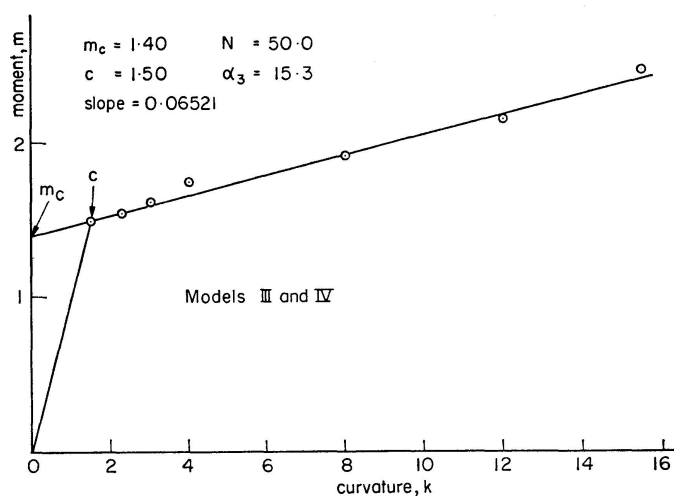


Fig. 6b. Cyclic Moment-Curvature Characteristics; Models III and IV.

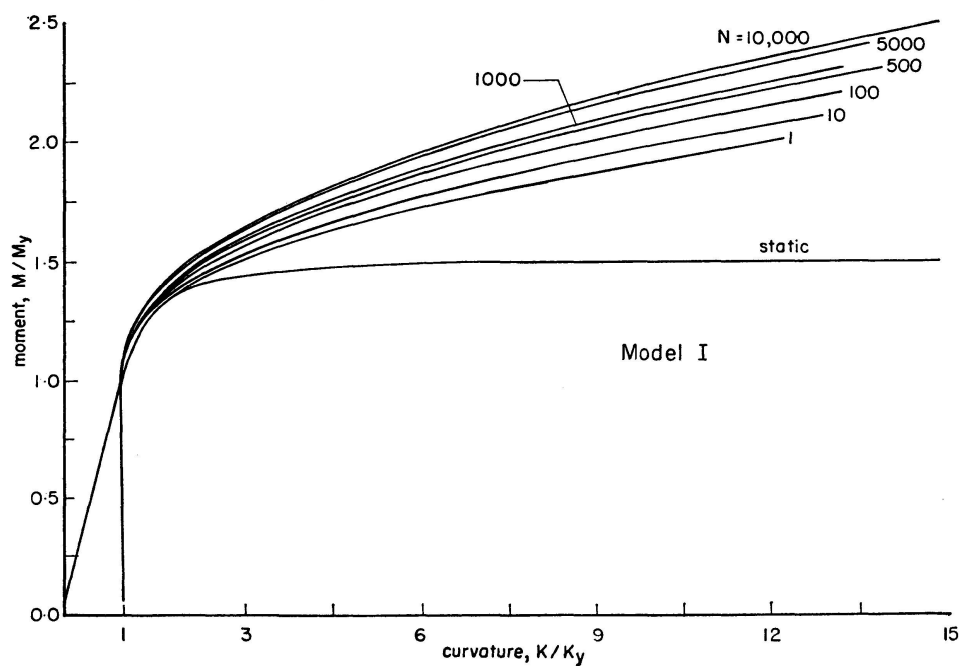


Fig. 7a. Cyclic Moment-Curvature Characteristics for Various Cycles: Model I.



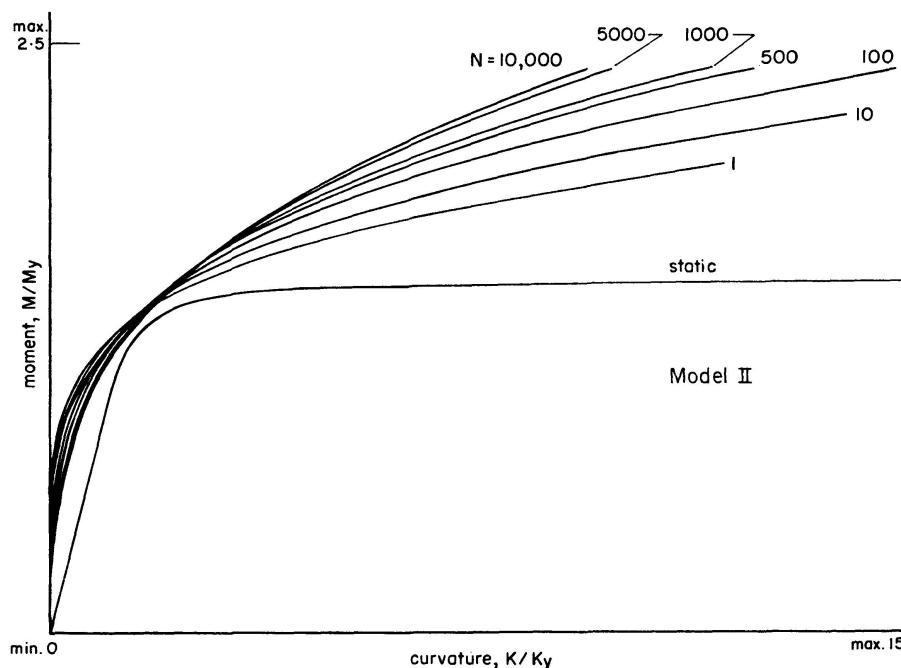


Fig. 7b. Cyclic Moment-Curvature Characteristics for Various Cycles: Model II.

cular cycle. In general, the experimental plots show linearity on log scales of  $m$  and  $k$  values; the curve II shows linearity on log scales of  $(m - 1)$  and  $(k - 1)$  values. This approximation may introduce an error and its magnitude will be comparatively greater near the yield point than at larger values of  $m$  and  $k$ . From Fig. 6a, however, this difference seems to be insignificant and, therefore, the approximation is acceptable without introducing serious error in the calculations.

### Analysis of Structural Components

It is proposed to apply the moment-curvature relations generated from experiments to structures in order to predict the cyclic history of loading under a constant range of alternating deflections. The following assumptions are made in formulating the theoretical approach:

- (I) the structure consists of prismatic members with rectangular sections symmetrical about the natural axis,
- (II) plane sections remain plane during elastic and inelastic bending,
- (III) the effect of shear and normal force is ignored,
- (IV) instability is not considered to be a factor,
- (V) the cross section of the beam remains constant throughout its cyclic life.

The moment-curvature relations derived in the preceding pages are applied in the analysis of simple and indeterminate structural systems. The  $m-k$  characteristics (I and II) derived from pure bending tests are applied to all

systems whereas those derived from the push-pull tests and Models III and IV are applied to cantilever beams only since it is believed sufficient to compare some typical results rather than repeating all the problems.

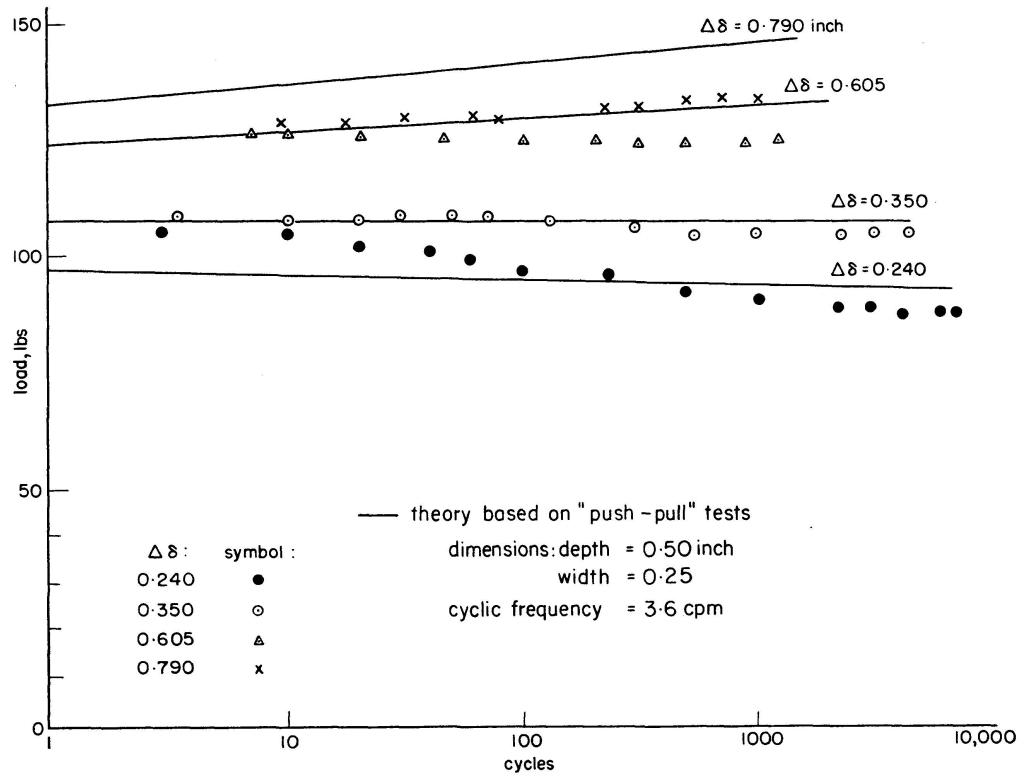


Fig. 8a.

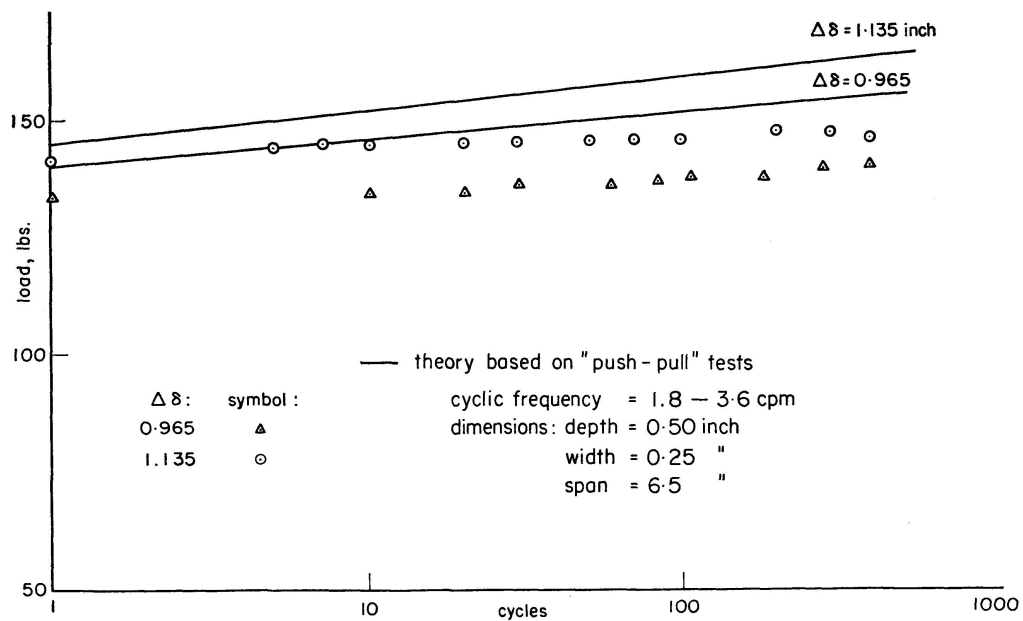


Fig. 8b.

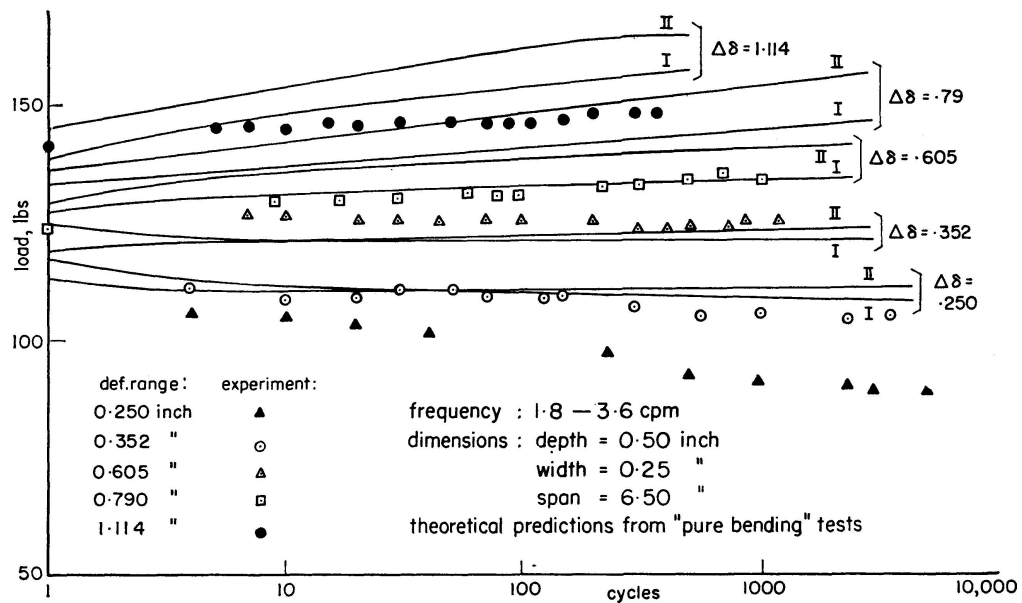


Fig. 8c.

Fig. 8a-c. Cyclic Variation of Load on Cantilever Beams under Constant Deflection Range.

### *Determinate Systems*

Simply supported and cantilever beams are analyzed theoretically and experimentally. Theoretical investigations and experimental procedures are reported in detail elsewhere [18, 19, 20].

The moment-curvature relations proposed above are applied here to predict the behaviour of simple determinate structures subjected to reversed bending under the constraint of a constant deflection range. The moment-area technique is applied to derive expressions for the angle change and tangential deviation

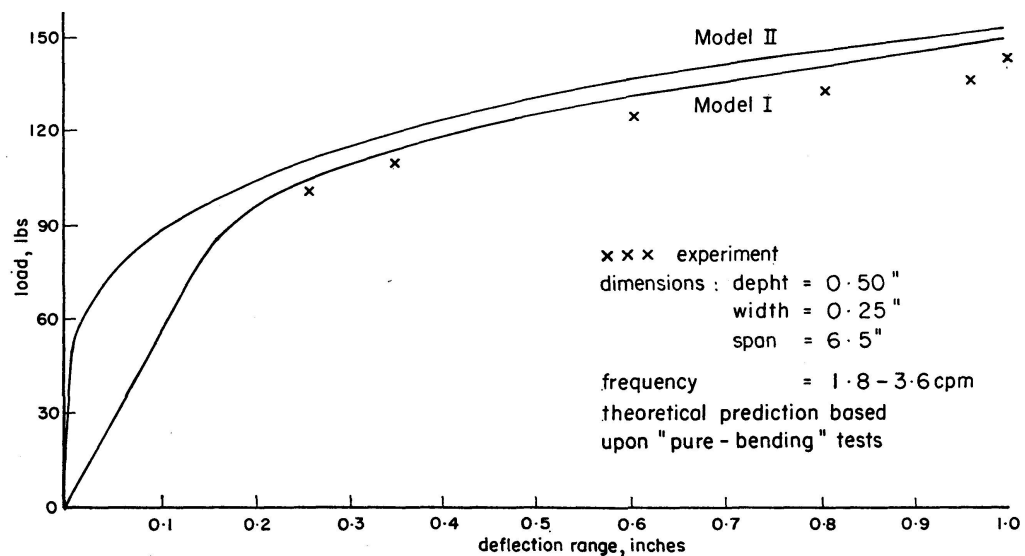


Fig. 9a. Cyclic Load-Deflection Range Curves for Cantilever Beams ( $N=50.0$ ): Models I and II.

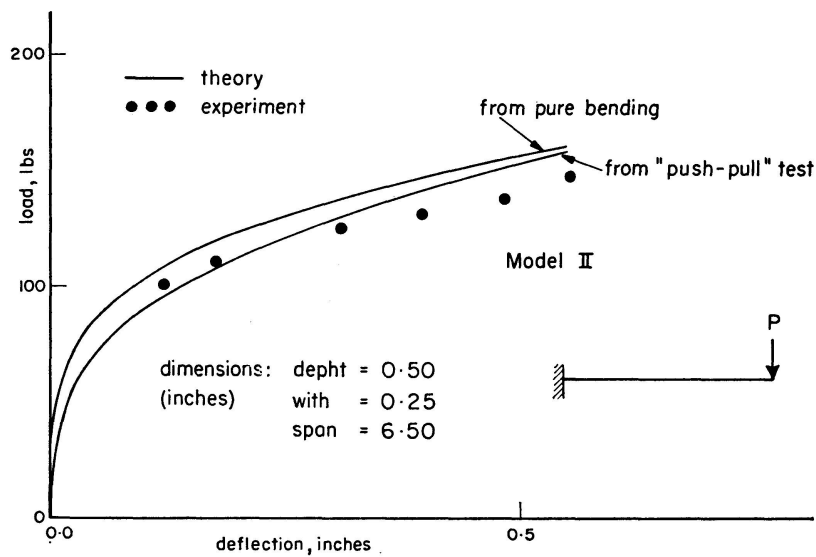


Fig. 9b. Cyclic Load-Deflection Curves for Cantilever Beams: Push-Pull and Pure Bending ( $N = 50.0$ ).

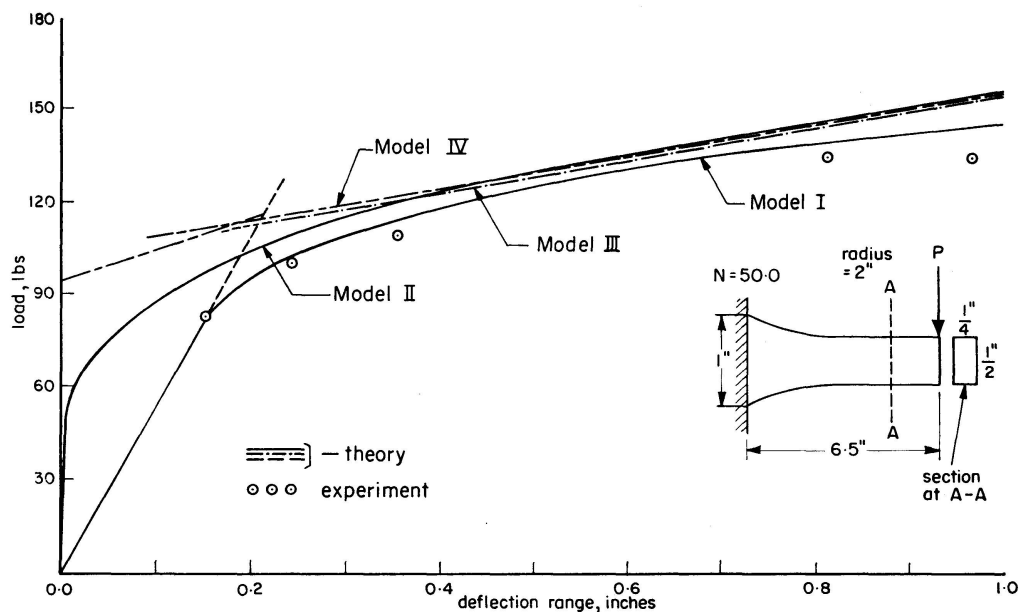


Fig. 9c. Cyclic Load-Deflection Range Curves for Cantilever Beams: Models I-IV.

of an element subjected to end moments. By suitably combining these expressions and applying the appropriate boundary conditions, the rotation and deformation of the structure at any point may be calculated (Appendix II).

Tests are carried out on eight  $6\frac{1}{2}$  inch long cantilever beam specimens measuring  $\frac{1}{2} \times \frac{1}{4}$  inch and  $\frac{1}{4} \times \frac{1}{4}$  inch. The deflection ranges are so chosen to cover the whole strain range possible, i.e., up to  $\pm 2.5\%$ . The frequency of the loading varies from 1.8 cpm. to 6 cpm. depending upon the deflection range. The computed results are plotted with the experimental values in Fig. 8. In Fig. 9, the load-deflection curves derived by applying both the moment-

curvature models, are plotted for one particular cycle along with the corresponding experimental results.

The analytical technique developed previously is now applied to predict the cyclic variation of loads on a simply supported beam subjected to a central load under a range of alternating deflection. Predicted values are compared with experiments after ROYLES [14]. The method is explained in detail in a paper by the authors [18] and the cyclic moment-curvature constant are given in Table 1b. The results are plotted in Fig. 10. The value of  $\epsilon_y$  is 0.13% for the material used by ROYLES [14].

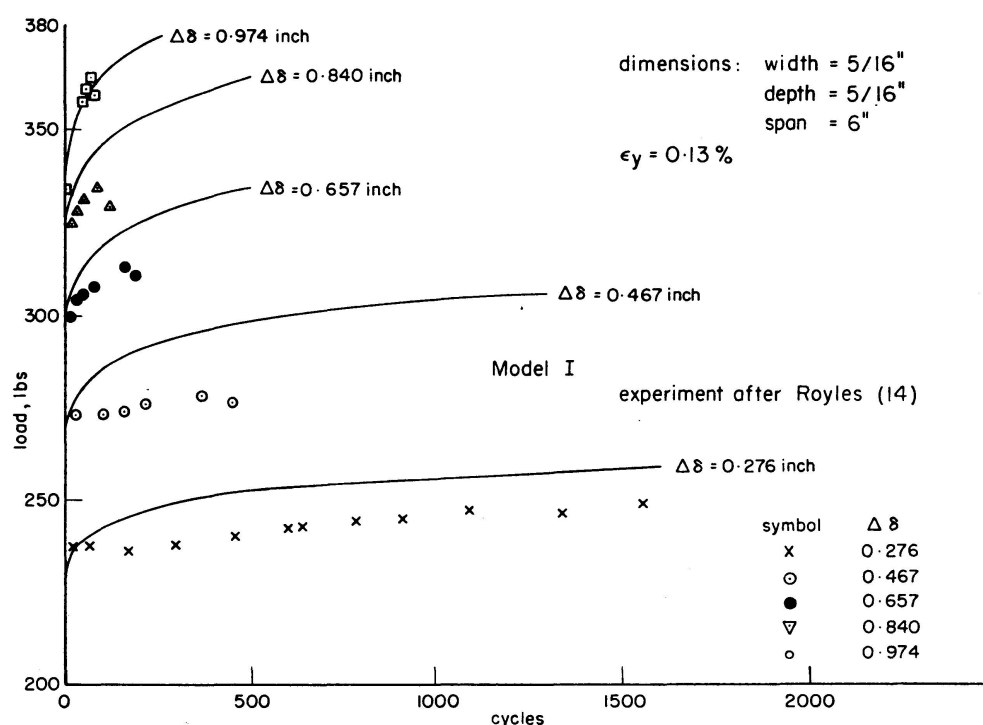


Fig. 10. Cyclic Variation of Load on Simple Beams under Constant Deflection Range (Model I).

### *Indeterminate Systems*

Analytical investigations are carried out on some indeterminate structures in order to predict their behaviour under a constant deflection range. One, two and three hinges systems are analyzed and the cyclic moment-curvature relationships (Models I and II) derived previously are employed in the calculations. A three-span continuous beam loaded symmetrically is analyzed and the predictions are compared with experiments after ROYLES [14]. Virtual work methods are employed in the analytical calculations (Appendix III) which are reported in detail elsewhere [20]. Load deflections curves (Figs. 11, 12 and 13) are plotted for various numbers of cycles of loading along with static load-deflection curves premised upon the usual bi-linear elastic-plastic moment-curvature relationship. In the two hinge system, the effect of varying

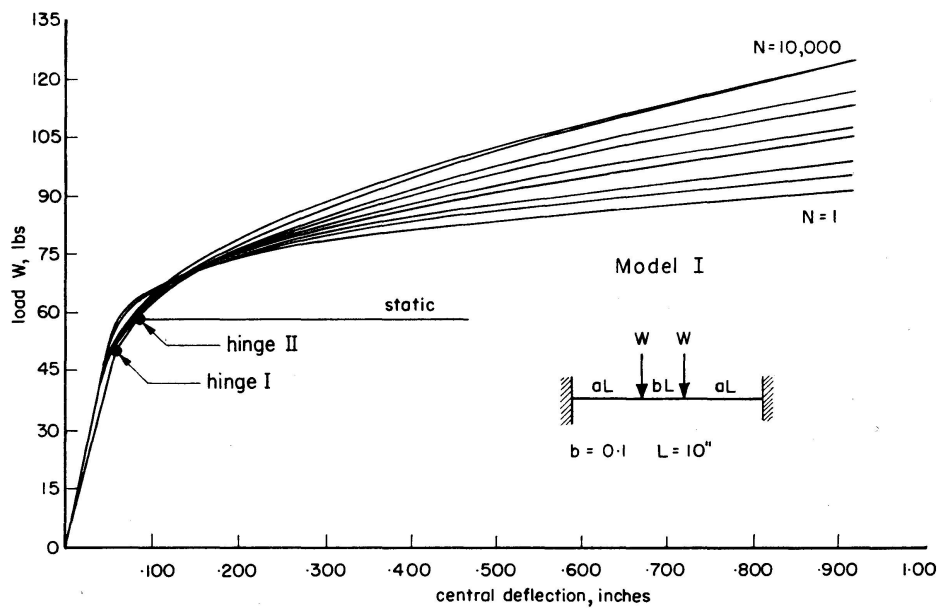


Fig. 11a. Cyclic Load-Deflection Curve for Two Hinge System: Model I.

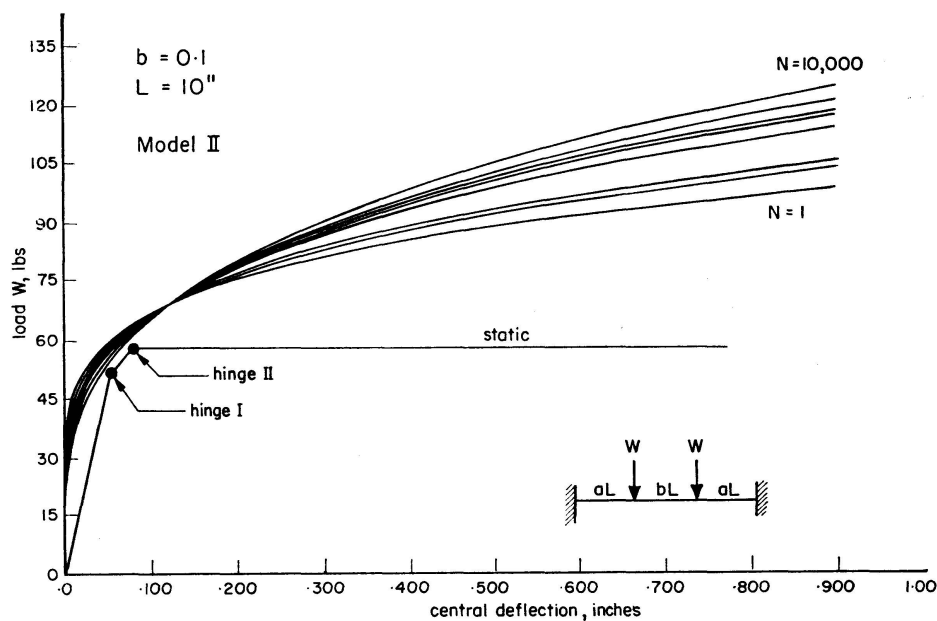


Fig. 11b. Cyclic Load-Deflection Curve for Two Hinge System: Model II.

the spacing between the two point loads is studied. For the centrally loaded continuous beam (Fig. 13), the cyclic variation of central bending moment for various deflection ranges is plotted in Fig. 14 along with experimental values of ROYLES [14]. The deflection ranges are maximum amplitudes of total 0.154, 0.243, 0.364, 0.554 and 0.740 inch equally divided in positive and negative curvature about the undisturbed reference position of the beams.

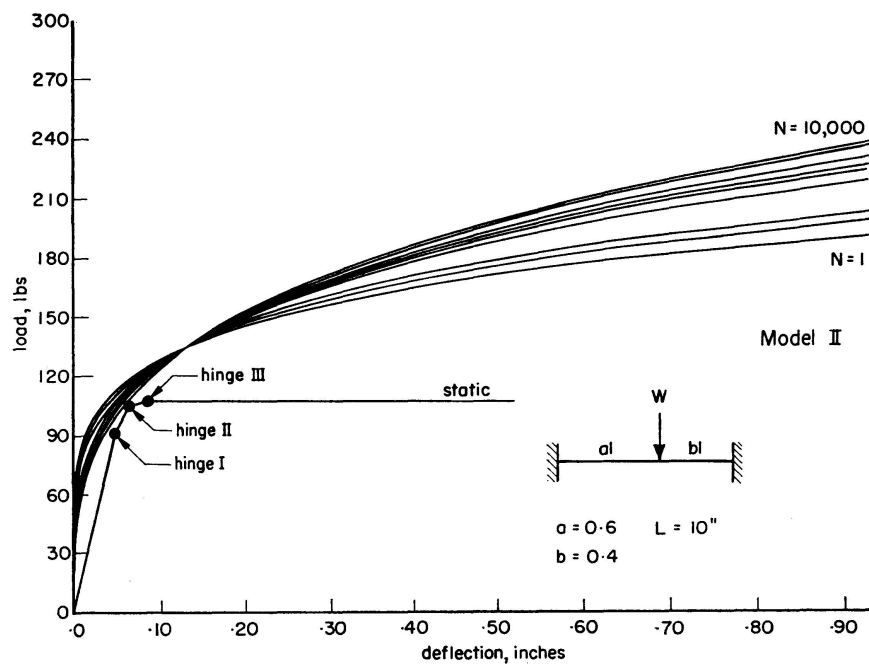


Fig. 12. Cyclic Load-Deflection Curve for Three Hinge System: Model II.

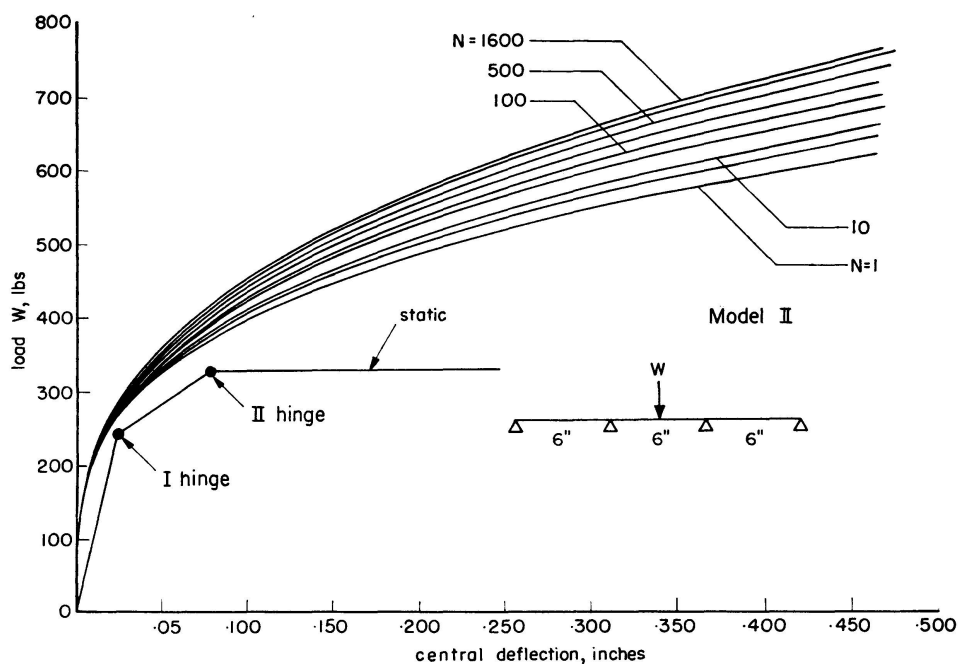


Fig. 13a. Cyclic Load-Deflection Curve for Continuous Beam: Model I.

Table 3a

System	Load (lbs)	Spacing of Loads	Span $L$ (inches)	Deflection Range
Single Hinge	160	—	—	—
Two Hinge	162	0.05 $L$	10	$\pm 0.5$ in.
	166	0.1 $L$	in all	in all
	187	0.2 $L$	the	the
	214	0.3 $L$	cases	cases

Table 3b

System	Load (lbs)		Spacing of Loads	Span $L$ (inches)	Deflection Range
	$N=1$	$N=10,000$			
Single Hinge	160	196	0		
Two Hinge	162	199	0.05 $L$	10	$\pm 0.5$ in.
	166	207	0.1 $L$	in all	in all
	187	229	0.2 $L$	the	the
	214	259	0.3 $L$	cases	cases

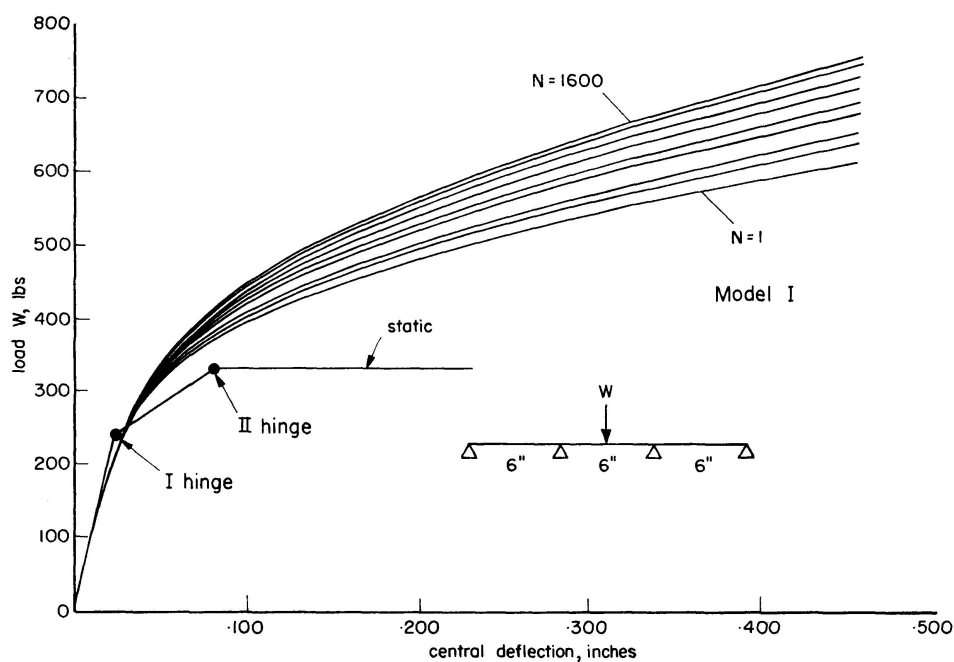


Fig. 13b. Cyclic Load-Deflection Curve for Continuous Beam: Model II.

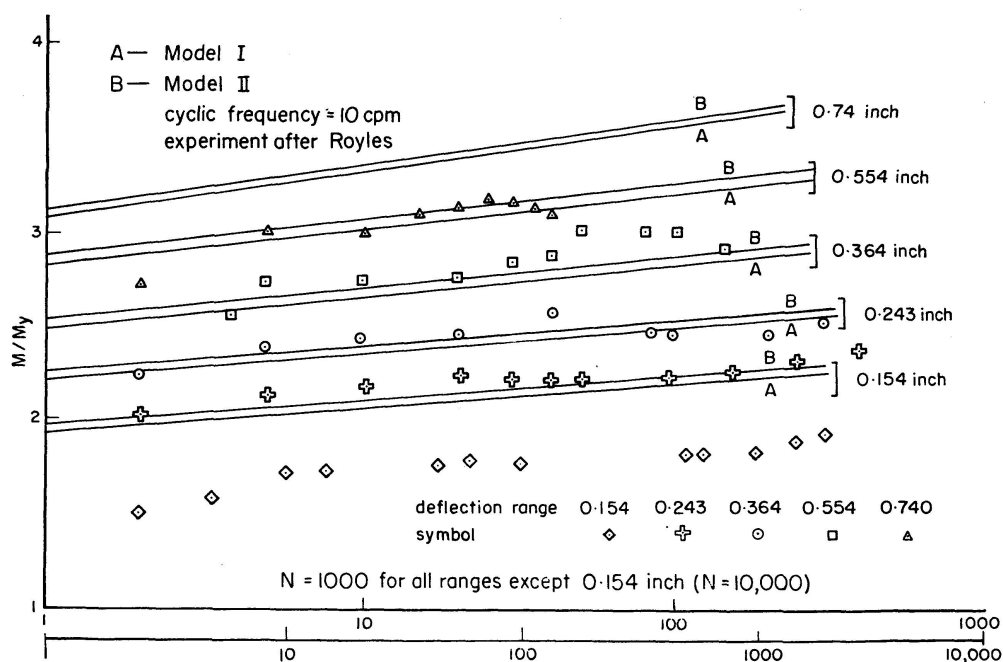


Fig. 14. Cyclic Variation of Central Bending Moment on Continuous Beam.



### Discussion and Conclusions

A method is developed for determining the cyclic variation of loads on simple and indeterminate beams subjected to a constant range of alternating deflection. Cyclic moment-curvature relations are generated from experiments involving pure bending and axial push-pull tests. Employing these moment-curvature characteristics, theoretical values of load variations on simple beams subjected to a constant range of reverse deflection are compared with tests.

Two types of moment-curvature relations are employed, designated as Model I and Model II, depending upon the inclusion or rejection of elastic strain components in the range of total strain. It follows, in general, that Model I will yield values closer to experiments than Model II. In the higher ranges of strain, however, where the effects of plastic strain dominate the two predictions are almost identical implying that the simpler continuous non-linear model can often be employed in the analysis of structures where elastic strains are small compared with plastic strains.

A bi-linear moment-curvature model (Model III) with two different slopes may be employed instead of Model I; it will yield a higher envelope to the problem but the calculations will be simplified to a significant extent. When the elastic and plastic strains are comparable, the error will be appreciable and this will become very small as the plastic strain increases with respect to the elastic strain.

A rigid strain hardening type of moment-curvature model (Model IV) can also be employed in the calculation, but, since the contribution due to the elastic component is neglected, the error in the working range (where the strains are very small) may be serious.

It is useful to suggest here that more experimental evidence in the yield region will give a better understanding of the nature of the behaviour of the material in order that a more realistic model might be assumed. Even though Model I is more cumbersome in its application, this can be overcome by the use of digital computers. It is also proved in general that the existing classical static analysis of structures is conservative.

The analysis presented in this paper predicts the load-response on the basis of certain moment-curvature data generated by recourse to simple tests, and  $m-k$  models derived from a fundamental stress-strain curve which is itself a function of the strain. The correlation seems to be good. The study reported here predicts the load-response of simple and indeterminate structures subjected to constant deflection range. The work will only be complete, and more practical, if it is also extended to embrace the behaviour of structural components under a constant load range. It will also be more correct if every point on the moment-curvature model is determined from a number of tests rather than a single test.

## Notations

$m$	moment amplitude
$m_e$	moment amplitude in the elastic range
$m_y$	yield moment
$N$	number of cycles
$k$	non-dimensional curvature (ratio between curvature at any point and that at yield)
$m$	non-dimensional moment (ratio between moment amplitude and that at yield)
$\alpha_1, \alpha_2, \alpha_3, \alpha_4, \beta_1, \beta_2, m_e, C$	constants of the moment-curvature relationship
$\Delta \epsilon$	strain range
$\theta$	angle change
$\delta$	tangential deviation
$\gamma, \Delta$	non-dimensional form of $\theta$ and $\delta$
$\phi_n$	end slope
$y_n$	deflection at a point
$y_c$	central deflection
$Y$	non-dimensional form of deflection
$\Delta_y$	deflection range
$L$	length of the beam
$S_1 \dots S_n$	segment lengths
$L_1 \dots L_n$	ratios: $\frac{S}{L} \dots \frac{S_n}{L}$
$I$	second moment of inertia
$E$	modulus of elasticity
$e$	extent of elastic region
$p$	extent of plastic region
$K_1, K_2$	constants
$\epsilon_y$	yield strain
$\Delta \epsilon$	strain range
$\Delta \sigma$	stress range
$\Delta \epsilon_m$	maximum strain range
$B$	width of the rectangular beam
$2d$	depth of the rectangular beam
$\sigma_y$	yield stress
$A, B, a, b$	material constants

## Appendix I. Cyclic Moment-Curvature Characteristics from Push-Pull Tests

The cyclic stress-strain range relationship can be represented by a polynomial as below:

$$\Delta \sigma = a (\Delta \epsilon)^b,$$

where  $a$ ,  $b$  are material constants (Table 2a).

Now the above stress-strain range relation is applied for deriving the cyclic moment-curvature characteristics for a symmetrical (rectangular) section.

The resisting moment of the section, then, can be written as:

$$M = 2 B \int_0^d \sigma x dx.$$

Evaluating the integral

$$M = \frac{B a}{2+b} \left( \frac{\Delta \epsilon_m}{d} \right)^b d^{(2+b)}. \quad (\text{I-1})$$

In the elastic range,  $a = E$  and  $b = 1$ . Hence, the value of the moment in the elastic range

$$M_e = \frac{B E}{3} \Delta \epsilon_m d^2$$

and the yield moment

$$M_y = \frac{2 B \sigma_y d^2}{3} \quad \text{where } \Delta \epsilon_m E = 2 \sigma_y.$$

Now rendering the yield (I-1) non-dimensional

$$m = \frac{M}{M_y} = \frac{3 a (\Delta \epsilon_m)^b}{2 (2+b) \sigma_y}. \quad (\text{I-2})$$

The moment-curvature characteristics can be plotted from Eq. (I-2) for various cycles by plugging the proper values of  $a$  and  $b$  and putting  $\sigma_y = 33.5 \cdot 10^3$  psi.

The  $m-k$  relationship employed in this paper is in the following form:

$$k = \alpha_2 (m)^{\beta_2},$$

where  $\alpha_2$ ,  $\beta_2$  are geometrical constants. Values of  $k$  and  $m$  are generated for a particular cycle from Eq. (I-2) and they are plotted on log-log scale (which as indicated earlier is a straight line) to arrive at the constants  $\alpha$  and  $\beta$ . This procedure is repeated for various cycles and the constants are tabulated (Table 2b).

## Appendix II. Deflection of Determinate Structures under Cyclic Loading [18]

Expressions are developed for angle changes and tangential deviations for various types of loadings on beam elements; these are applied to predict the variation of load on simple beams subjected to a constant range of alternating deflection.

*Inelastic Bending Relationships*

As explained earlier, four types of moment-curvature relations (Eq. 1 to 4) are employed in the analytical computations. Here, relationships are developed for the first two models under various loadings and are tabulated in Table 4. The relationships for the other two models can be similarly derived.

Table 4

	$\nu$ = Rotation			
	$m_1 < 1.0$ $m_2 > 1.0$	$m_1 \geq 1.0$ $m_2 < 1.0$	$m_1 \geq 1.0$ $m_2 > 1.0$	$m_1 = m_2$
Elastic Non-Linear	$A + C + D$	$A + C - D$	$C + H + 1.0$	$1.0 + \alpha_1 (m_1 - 1)^{\beta_1}$
Complete Non-Linear	$\frac{\alpha_2 \{m_2^{(\beta_2+1)} - m_1^{(\beta_2+1)}\}}{(\beta_2 + 1)(m_2 - m_1)}$			$\alpha_2 (m_1)^{\beta_2}$
Elastic	$A$			
	$\Delta$ = Tangential Deviation			
	$m_1 < 1.0$ $m_2 > 1.0$	$m_1 \geq 1.0$ $m_2 < 1.0$	$m_1 \geq 1.0$ $m_2 > 1.0$	$m_1 = m_2$
Elastic Non-Linear	$B + E - F$	$H - G + F$	$E - G + H + 0.5$	$\nu/2$
Complete Non-Linear	$\frac{\alpha_2 \{m_2^{(\beta_2+2)} - m_1^{(\beta_2+2)}\}}{(\beta_2 + 1)(\beta_2 + 2)(m_2 - m_1)^2} - \frac{\alpha_2 (m_1)^{(\beta_2+1)}}{(\beta_2 + 1)(m_2 - m_1)}$			$\nu/2$
Elastic	$B$			

$$\begin{aligned}
 A &= (m_1 + m_2)/2; & B &= (2m_1 + m_2)/6; & C &= \{\alpha_1 (m_2 - 1)^{\beta_1+1}\} / \{(\beta_1 + 1)(m_2 - m_1)\}; \\
 D &= (m_2 - 1)^2/2(m_1 - m_2); & E &= \{\alpha_1 (m_2 - 1)^{\beta_1+2}\} / \{(\beta_1 + 1)(\beta_1 + 2)(m_2 - m_1)^2\}; \\
 F &= \{(m_2 - 1)^3\} / \{6(m_2 - m_1)^2\}; & G &= \{\alpha_1 (m_1 - 1)^{\beta_1+2}\} / \{(\beta_1 + 1)(\beta_1 + 2)(m_1 - m_2)^2\}; \\
 H &= \{\alpha_1 (m_1 - 1)^{\beta_1+1}\} / \{(\beta_1 + 1)(m_1 - m_2)\}.
 \end{aligned}$$

*1. Model I*

Using the appropriate relationship (Eq. 1), angle changes and tangential deviations of flexural members may be determined by direct integration:

Elastic Region

$$\begin{aligned}
 \theta_{AB} &= K_y L \int_A^B k d(x/L) = \frac{M_y L}{EI} \int_A^B m d(x/L), \\
 \delta_{BA} &= K_y L^2 \int_A^B k(x/L) d(x/L) = \frac{M_y L^2}{EI} \int_A^B m(x/L) d(x/L).
 \end{aligned} \tag{II-1}$$

Inelastic Region

$$\theta_{AB} = K_y L \int_A^B k d(x/L) = \frac{M_y L}{EI} \int_A^B m d(x/L) + \frac{M_y L}{EI} \int_A^B \{1.0 + \alpha_1 (m-1)^{\beta_1}\} d(x/L),$$

$$\delta_{BA} = K_y L^2 \int_A^B k(x/L) d(x/L) = \frac{M_y L^2}{EI} \int_A^B m(x/L) d(x/L) \quad (\text{II-2})$$

$$+ \frac{M_y L^2}{EI} \int_A^B \{1.0 + \alpha_1 (m-1)^{\beta_1}\} (x/L) d(x/L).$$

where  $\theta_{AB}$  = total angle change between two points  $A$  and  $B$ .

$\delta_{BA}$  = the tangential deviation of point  $A$  from the tangent through point  $B$ ; distance  $(x/L)$  is measured from  $A$ .

## 2. Model II

Applying the Model II type of moment-curvature relationship (Eq. 2), the expressions for  $\theta$  and  $\delta$  are as follows:

$$\theta_{AB} = K_y L \int_A^B k d(x/L) = \frac{M_y L}{EI} \int_A^B \alpha_2 (m)^{\beta_2} d(x/L), \quad (\text{II-3})$$

$$\delta_{BA} = K_y L^2 \int_A^B k(x/L) d(x/L) = \frac{M_y L^2}{EI} \int_A^B \alpha_2 (m)^{\beta_2} (x/L) d(x/L).$$

### Expressions for $\theta$ and $\delta$

Considering the beam element subjected to a load as shown in Fig. 15, the angle change and tangential deviation can be obtained by employing the appropriate equations (II-1) to (II-3) above. All values are made dimensionless for convenience.

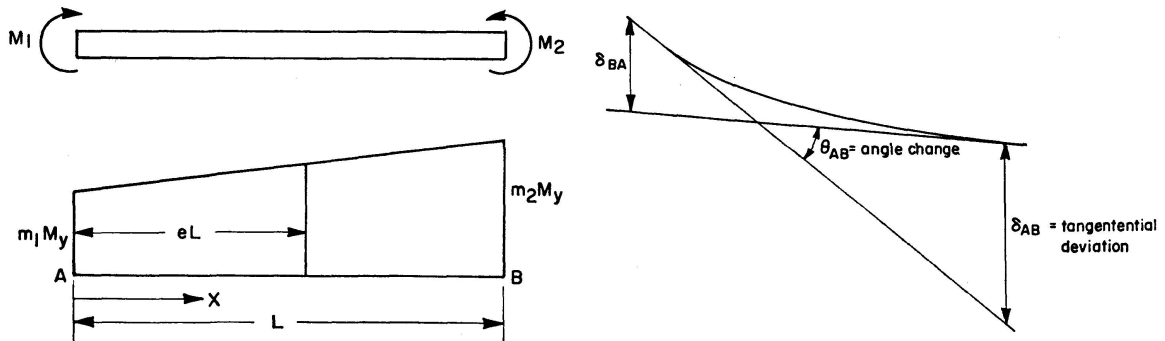


Fig. 15. Beam Element.

## 1. Model I

*I. Angle Change.* Moment at any point,  $x/L$  (taking the origin at  $A$ )

$$m_{(x/L)} = m_1 + (m_2 - m_1) (x/L). \quad (\text{II-4})$$

In the elastic region,

$$k_{(x/L)} = m_1 + (m_2 - m_1) (x/L) \quad (\text{II-5})$$

and in the inelastic region,

$$k_{(x/L)} = 1.0 + \alpha_1 \{m_1 + (m_2 - m_1) (x/L) - 1.0\}^{\beta_1}. \quad (\text{II-6})$$

The change in angle between  $A$  and  $B$ , from expressions (II-5) and (II-6), is:

$$\begin{aligned} \theta_{AB} = & \frac{M_y L}{E I} \int_0^e \{m_1 + (m_2 - m_1) (x/L)\} d(x/L) \\ & + \frac{M_y L}{E I} \int_e^{1.0} [1.0 + \alpha_1 \{m_1 + (m_2 - m_1) (x/L) - 1.0\}^{\beta_1}] d(x/L). \end{aligned} \quad (\text{II-7})$$

By evaluating the integral (II-7)

$$\theta_{AB} = \frac{M_y L}{E I} \left\{ \frac{m_1 + m_2}{2} + \frac{\alpha_1 (m_2 - 1.0)^{(\beta_1+1)}}{(\beta_1 + 1)(m_2 - m_1)} - \frac{(m_2 - 1)^2}{2(m_2 - m_1)} \right\} = \gamma \frac{M_y L}{E I}. \quad (\text{II-8})$$

*II. Tangential Deviation.* One needs the tangential deviation  $\delta_{AB}$ ; this can be determined by applying expression (II-2) in which the origin is taken at point  $B$  instead of  $A$ . The moment at any point  $(x/L)$  is thus given by:

$$m_{(x/L)} = m_2 - (m_2 - m_1) (x/L). \quad (\text{II-9})$$

The tangential deviation becomes:

$$\begin{aligned} \delta_{AB} = & \frac{M_y L^2}{E I} \int_0^p [1.0 + \alpha_1 \{m_2 - (m_2 - m_1) (x/L)^{\beta_1}\}] (x/L) d(x/L) \\ & + \frac{M_y L^2}{E I} \int_p^{1.0} \{m_2 - (m_2 - m_1) (x/L)\} (x/L) d(x/L). \end{aligned} \quad (\text{II-10})$$

Evaluation of the integral (II-10) leads to:

$$\delta_{AB} = \frac{M_y L^2}{E I} \left\{ \frac{2m_1 + m_2}{6} + \frac{\alpha_1 (m_2 - 1)^{(\beta_1+2)}}{(\beta_1 + 1)(\beta_1 + 2)(m_2 - m_1)^2} - \frac{(m_2 - 1)^3}{6(m_2 - m_1)^2} \right\} = \Delta \frac{M_y L^2}{E I}. \quad (\text{II-11})$$

## 2. Model II

*I. Angle Change.* Moment at any point  $(x/L)$  (origin at  $A$ )

$$m_{(x/L)} = m_1 + (m_2 - m_1) (x/L). \quad (\text{II-12})$$

Then

$$k_{(x/L)} = \alpha_2 \{m_1 + (m_2 - m_1) (x/L)\}^{\beta_2}. \quad (\text{II-13})$$

Change in angle

$$\begin{aligned}\theta_{AB} &= \frac{M_y L}{EI} \int_0^{1.0} \alpha_2 \{m_1 + (m_2 - m_1)(x/L)\}^{\beta_2} d(x/L) = \\ &= \frac{M_y L}{EI} \frac{\alpha_2 \{m_2^{(\beta_2+1)} - m_1^{(\beta_2+1)}\}}{(\beta_2 + 1)(m_2 - m_1)} = \gamma \frac{M_y L}{EI}.\end{aligned}\quad (\text{II-14})$$

II. *Tangential Deviation.* Moment at any point  $(x/L)$  with origin at  $B$

$$m_{(x/L)} = m_2 - (m_2 - m_1)(x/L). \quad (\text{II-15})$$

Then

$$k_{(x/L)} = \alpha_2 \{m_2 - (m_2 - m_1)(x/L)\}^{\beta_2}. \quad (\text{II-16})$$

Tangential deviation

$$\begin{aligned}\delta_{AB} &= \frac{M_y L^2}{EI} \int_0^{1.0} \alpha_2 \{m_2 - (m_2 - m_1)(x/L)\}^{\beta_2} (x/L) d(x/L) = \\ &= \frac{M_y L^2}{EI} \left[ \frac{\alpha_2 \{m_2^{(\beta_2+2)} - m_1^{(\beta_2+2)}\}}{(\beta_2 + 1)(\beta_2 + 2)(m_2 - m_1)^2} - \frac{\alpha_2 (m_1)^{\beta_2+1}}{(\beta_2 + 1)(m_2 - m_1)} \right] = \Delta \frac{M_y L^2}{EI}.\end{aligned}\quad (\text{II-17})$$

As explained above, the expressions for the values of  $\gamma$  and  $\Delta$  for various types of loadings are derived and tabulated (Table 4).

### Example

The above expressions are now applied to solve a particular problem. The method as explained in this paper is oriented to a digital computer since the amount of work is enormous and it is cumbersome to do by hand. A detailed study of the computer flow diagram [18] indicates that, in order to proceed with the solution of the problem, it is necessary to know two initial conditions of either of the boundaries, i.e., rotation and deflection at the support. In a cantilever beam, for example, the values of  $\phi$  and  $y$  are known at the built-in end. In the case of a simply supported beam, however, only  $y$  is known and  $\phi$  has to be determined at the support. It is, therefore, proposed to formulate an expression for the end slope  $\phi$  of a simple supported beam in terms of the constants  $\gamma$  and  $\Delta$ .

A simply supported beam loaded as shown in Fig. 16 is considered. The solution is first formulated for this particular problem and is then generalized for any type of loading.

The B.M. diagram is drawn for the given loading and divided into as many small parts as required; the ordinates are designated as shown.

Constants  $\gamma_1, \gamma_2, \gamma_3$  and  $\Delta_1, \Delta_2, \Delta_3$  are the values of  $\gamma$  and  $\Delta$  for the segments (1)–(2), (2)–(3) and (3)–(4), respectively.

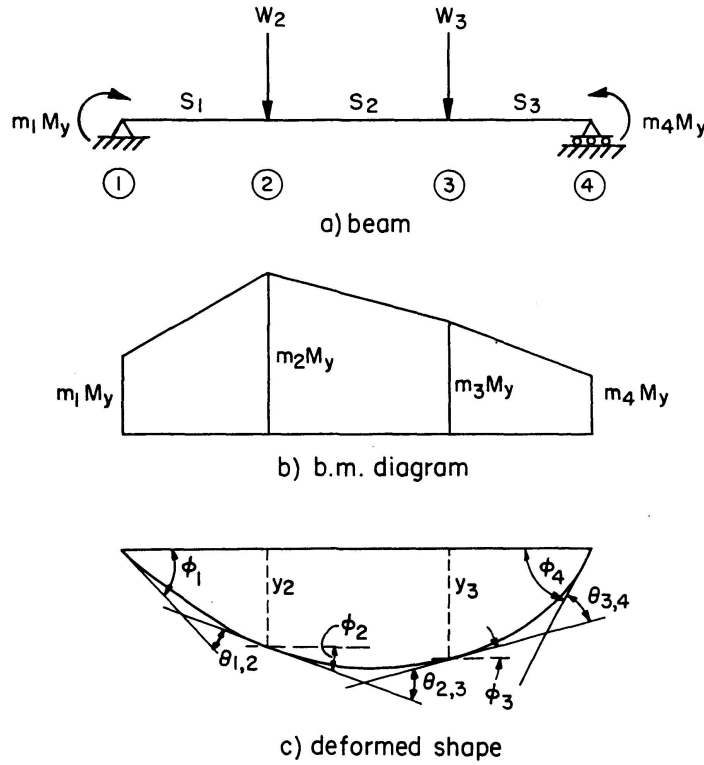


Fig. 16. Simple Beam (Example).

From Fig. 16, a general expression for  $\phi$  can be derived as shown below:

$$\begin{aligned} \phi = & \frac{M_y L}{EI} \{ \gamma_1 L_1 + \gamma_2 L_2 + \gamma_3 L_3 + \cdots + \gamma_{n-1} L_{n-1} \} \\ & + \frac{M_y L}{EI} [ \{ \Delta_1 L_1^2 + \Delta_2 L_2^2 + \cdots + \Delta_{n-1} L_{n-1}^2 \} \\ & - \{ \gamma_1 L_1 L_1 + \gamma_2 (L_1 + L_2) L_2 + \cdots + \gamma_{n-1} (L_1 + L_2 + \cdots + L_{n-1}) L_{n-1} \} ]. \end{aligned} \quad (\text{II-18})$$

In order to solve a specific problem applying the above technique, the following steps are necessary:

1. The bending moment diagram for the given loading is drawn and is divided into as many segments as necessary. Each ordinate of the diagram is divided by the yield moment ( $M_y$ ) to make it dimensionless.
2. The constants  $\alpha$  and  $\beta$  are chosen for a particular cycle of loading.
3. The values of  $\gamma$  and  $\Delta$  are evaluated for all the segments of the beam by applying the appropriate expression.
4. Using the expression (II-18) the value of  $\phi_1$  is calculated.
5. Once  $\phi_1$  is known, it is a simple addition and subtraction, using values of  $\gamma$  and  $\Delta$ , to calculate the rotation and deflection of the beam at any required point.
6. The procedure may be repeated for any number of cycles.



The above technique can be made more convenient to apply in the solution of problems by plotting values of  $m_2$  against  $\gamma$  and  $\Delta$  for various values of  $m_1$ . In order to solve a problem completely, one needs a family of plots for all loading cycles.

The procedure explained above is easy to apply in finding the rotations and deformations of a beam once the load is defined. When it is required to find the loads on the beam for a given deflection, it becomes cumbersome and a trial and error procedure has to be invoked. To avoid this difficulty a digital computer programme is developed in the language of Fortran II [18]. This programme will compute the loads on a determinate structure for a given deflection by properly reading in some specific initial conditions.

### Appendix III. Central Deflection of Two Hinge System

Typical calculations for a two hinge system are shown. The moment-curvature relationship (Model I) is used in the calculations. Due to symmetry of loading, there is only one unknown, the end moment. Assuming that the ratio between the moment at the loading point and the end moment is equal to  $\kappa$ , the expression for the end moment can be written in terms of  $\kappa$ ,  $a$  and  $W$  as shown below.

Referring to Fig. 17,

$$m - \frac{W a L}{M_y} = -\kappa m \quad (\text{III-1})$$

or

$$m = \frac{W a L}{(\kappa + 1) M_y}.$$

If the value of the constant  $\kappa$  is known for a given value of  $W$ , the value of  $m$  can be evaluated from equation (III-1). The value of  $\kappa$  can be found from virtual work equations [21].

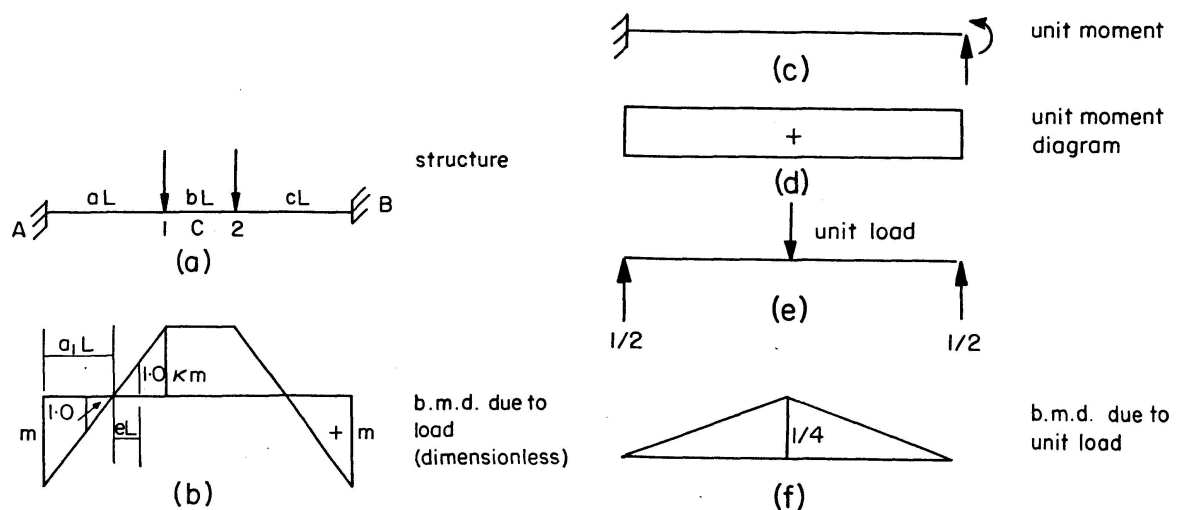


Fig. 17. Two Hinge System.

There are three stages of loading:

1. purely elastic,
2. the moment at  $A$  exceeds the elastic limit but the moment at  $I$  is below the yield point, i. e.  $m > 1.0$  and  $\kappa m \leq 1.0$ ,
3. moment at  $A$  and  $I$  exceed the elastic limit.

It should be noted here that the loading on the structure is assumed such that the points  $A$  and  $B$  reach the yield limit before any other point on the structure. The deflection of the beam at the centre can be calculated by writing the virtual work equation. Here three cases mentioned above have to be considered. The equation for deflection in each case is derived by knowing the values of  $\kappa$  and appropriately combining the loadings (Figs. 17b and 17f).

A detailed derivation of these equations is given in Ref. [21].

*Stage (I)* ( $m \leq 1.0$  and  $\kappa m < 1.0$ )

$$y_c = \frac{M_y L^2}{EI} \left[ -\frac{m a_1^2}{6} + \frac{\kappa m (a - a_1) (2a + a_1)}{6} + \frac{\kappa m (1 - 4a^2)}{8} \right]. \quad (\text{III-2})$$

*Stage (II)* ( $m > 1.0$  and  $\kappa m < 1.0$ )

$$y_c = \frac{2 M_y L^2}{EI} \left[ -\left\{ \frac{(a_1 - e)^2}{4} + \frac{\alpha_1 a_1^2 (m - 1)^{\beta_1 + 2}}{2 (\beta_1 + 1) (\beta_1 + 2) m^2} \right\} - \left\{ \frac{m}{4} [a_1^2 - (a_1 - e)^2] \right. \right. \\ \left. \left. - \frac{m}{6 a_1} [a_1^3 - (a_1 - e)^3] \right\} + \frac{\kappa m (a - a_1) (2a + a_1)}{12} + \frac{\kappa m (1 - 4a^2)}{16} \right]. \quad (\text{III-3})$$

*Stage (III)* ( $m > 1.0$  and  $\kappa m > 1.0$ )

$$y_c = \frac{2 M_y L^2}{EI} \left[ -\left\{ \frac{(a_1 - e)^2}{4} + \frac{\alpha_1 a_1^2 (m - 1)^{\beta_1 + 2}}{2 (\beta_1 + 1) (\beta_1 + 2) m^2} \right\} - \left\{ \frac{m}{4} [a_1^2 - (a_1 - e)^2] \right. \right. \\ \left. \left. - \frac{m}{6 a_1} [a_1^3 - (a_1 - e)^3] \right\} + \frac{a - a_1}{2 \kappa m} \left\{ \frac{a_1}{2} + \frac{a - a_1}{3 \kappa m} \right\} \right. \\ \left. + \left\{ \frac{(a - a_1)^2 (\kappa m - 1) + (\kappa m - 1) (a^2 - a_1^2)}{4 \kappa^2 m^2} + \frac{\alpha_1 a (a - a_1) (\kappa m - 1)^{\beta_1 + 1}}{m (\beta_1 + 1)} \right. \right. \\ \left. \left. - \frac{\alpha (a - a_1)^2 (\kappa m - 1)^{\beta_1 + 2}}{\kappa^2 m^2 (\beta_1 + 1) \beta_1 + 2} \right\} + \{1 + \alpha_1 (\kappa m - 1)^{\beta_1}\} \left\{ \frac{1 - 4a^2}{16} \right\} \right]. \quad (\text{III-4})$$

Employing the moment-curvature Model II, the central deflection can be written as follows:

$$y_c = \frac{2 M_y L^2}{EI} \left[ -\frac{\alpha_2 a_1^2 m^{\beta_2}}{2 (\beta_2 + 1) (\beta_2 + 2)} + \frac{\alpha_2 (\kappa m)^{\beta_2} (a - a_1)}{2 (\beta_2 + 1) (\beta_2 + 2)} \{a_1 + a (\beta_2 + 1)\} \right. \\ \left. + \frac{\alpha_2 (\kappa m)^{\beta_2}}{16} (1 - 4a^2) \right]. \quad (\text{III-5})$$

### Acknowledgements

This investigation was carried out in the Department of Civil Engineering of the University of Waterloo under National Research Council of Canada Grant No. A-1582.

### References

1. SYMONDS, P. S., "Cyclic Loading Tests on Small Scale Portal Frames". Final Report, International Association for Bridge and Structural Engineering, 4th Congress, Cambridge and London, 1953.
2. SYMONDS, P. S., and NEAL, B. G., "Cyclic Loading of Portal Frames-Theory and Tests". Vol. 18, Pub. IABSE, Zurich, 1958.
3. MASSONNET, C., „Essais d'adaptation et de stabilisation plastique sur des poutrelles laminées“. *L'Ossature Métallique* (1954), No. 5, p. 318.
4. KLÖPPEL, K., „Beitrag zur Frage der Ausnutzbarkeit der Plastizität bei Dauerbeanspruchungen“. Final Report, 2nd Congress, IABSE (1939), p. 77.
5. GOZUM, A. T., and HAAIZER, G., "Deflection Stability (Shakedown) of Continuous Beams". Lehigh University Interim Report No. 28, 1965.
6. POPOV, E. P., and MCCARTHY, R. E., "Deflection Stability of Frames Under Repeated Loading". *Journal E. M. Division, ASCE*, January, 1960.
7. BENHAM, P. P., "Fatigue of Metals Caused by Relatively Few Cycles of High Load or Strain Amplitude". *Metallurgical Reviews*, Vol. 3, No. 11, p. 203-204, 1950.
8. DUGDALE, D. S., "Stress-Strain Cycles of Large Amplitudes". *Journal of Mechanics and Physics of Solids*, Vol. 7, p. 135-142, March 1959.
9. COFFIN, L. F., and TAVERNELLI, J. E., "The Cyclic Straining and Fatigue of Metals". *Met. Soc. AMIE Trans.*, 215, p. 794-807, October, 1959.
10. BENHAM, P. P., and FORD, H., "Low Endurance Fatigue of a Mild Steel and an Aluminium Alloy". *Journal of Mech. Eng. Science*, 3, No. 2, p. 119-132, June, 1961.
11. TOPPER, T. H., "Cyclic Plastic Loading of Mild Steel". Ph. D. Thesis, Cambridge University, England, 1962.
12. HORNE, M. R., "The Effect of Repeated Loads in Building Structures Designed by Plastic Theory". Vol. 14, Publication IABSE, Zurich, 1954.
13. PARKES, E. W., "Wings under Repeated Thermal Stress". *Aircraft Engineering* 26, p. 402, 1954.
14. ROYLES, R., "Fatigue of Ductile Structures in Reversed Bending". Ph. D. Thesis, Cambridge University, England, 1964.
15. SHERBOURNE, A. N., "Some Preliminary Experiments on the Behaviour of Ductile Structures under Repeated Loads". *Journal of the SESA*, Vol. 3, No. 5, p. 119, May, 1963.
16. BLATHERWICK, A. A., and LAZAN, B. J., "Effect of Changing Cyclic Modulus on Bending Fatigue Strength, WADC Technical Report 56-127, Part II, May, 1959.
17. KESHAVAN, S., "Some Studies on the Deformation and Fracture of Normalized Mild Steel under Cyclic Conditions". Ph. D. Thesis, University of Waterloo, Waterloo, Ontario, Canada, 1967.
18. KRISHNASAMY, S., and SHERBOURNE, A. N., "Mild Steel Structures under Reversed Bending". RILEM Symposium on the "Effects of Repeated Loading on Materials and Structures". Mexico City, 1966.
19. KRISHNASAMY, S., and SHERBOURNE, A. N., "Response of a 'Plastic Hinge' to Low Cycle Alternating Deflections". *Experimental Mechanics*, 8 (6), p. 241-248, 1968.

20. SHERBOURNE, A. N., and KRISHNASAMY, S., "Moment-Curvature Models under Reverse Cyclic Straining". *Experimental Mechanics* 9 (1), p. 36-40, 1969.
21. SHERBOURNE, A. N., and KRISHNASAMY, S., "Indeterminate Systems under Cyclic Loading". *Materials and Constructions (RILEM)*, Vol. 1, No. 4, 1968.

### Summary

An analytical technique, based upon some simple experiments, is developed for predicting the behaviour of mild steel, simple and indeterminate, structures subject to reversed bending of the type in which a strain (or deflection) range is prescribed. The method constructs moment-curvature relationships which are functions of the cyclic history of the structure and uses these curves to determine the variation of load with cyclic straining.

### Résumé

En se basant sur des expériences simples, on développe une méthode analytique pour prévoir les propriétés de structures en acier doux, simples et indéterminées sujettes à une contre-courbe du type dans lequel une classe de déformations (ou de flexion) est prescrite. La méthode conduit à des relations moment-courbure qui sont fonction du passé cyclique de la structure et utilise ces courbes pour déterminer la variation de la charge avec des contraintes cycliques.

### Zusammenfassung

Es wird auf Grund einiger einfacher Versuche ein Berechnungsverfahren entwickelt, um das Verhalten von Tragwerken aus normalem Baustahl, einfach und unbestimmt, unter durch den Dehnungs- oder Durchbiegungsbereich vorgeschriebener Wechselbiegung vorauszusagen. Die Methode ergibt Moment-Durchbiegungs-Beziehungen, die Funktionen der Wechselbelastung sind, und verwendet diese Kurven zur Bestimmung der Laständerung mit zyklischer Dehnung.

Leere Seite  
Blank page  
Page vide